

Quantum cooperative effects in a micromaser

Miguel Orszag and Ricardo Ramírez

Facultad de Física, Pontificia Universidad Católica de Chile, Casilla 306, Santiago, Chile

Juan C. Retamal and Carlos Saavedra

Departamento de Física, Universidad de Tarapacá, Casilla 7-D, Arica, Chile

(Received 15 October 1993)

We study the collective effects in the trapping states in a one-photon micromaser. We find that, for small photon numbers, the trapping states are difficult to detect experimentally due to these effects. On the other hand, for higher trapping conditions, the behavior of $\langle n \rangle$ is similar to the usual trapping states, except for the appearance of spikes and also large fluctuations of the photon number.

PACS number(s): 42.52.+x, 42.50.Dv

I. INTRODUCTION

Cooperative effects in a micromaser have been recently studied in a semiclassical regime for high fluxes [1]. The present paper deals with cooperative effects in a totally different context; namely, we analyze the effects of having, for a short while, two atoms at the same time inside the microwave cavity on the trapping states [2,3]. So, obviously, here we are dealing with quantum cooperative effects, which can be applied for both low or high atomic fluxes. We think that this may be of relevance for the experimental detection of the trapping states, since the atomic beams are distributed with a Poisson injection statistics [4]. Therefore, no matter how low the beam intensity is, there will always be a finite (nonzero) probability of simultaneously having two atoms. Naively thinking, one could say that besides the usual one-photon transition, the presence of a second atom will introduce two-photon transitions. Therefore, since both trapping conditions (the one and two photon) cannot be satisfied simultaneously, one would suspect that the trap will leak or that the system will stay in a trap for a while and then jump to the next trap with a higher photon number and so on. We find this to be the case, with the surprising fact that the effect is very strong even for probabilities of having two atoms of the order or less than 1%.

II. MODEL

Whenever two atoms are present in a microwave cavity, we can model this, in the dipole and rotating-wave approximation, by the following Hamiltonian:

$$H = \hbar\omega_0 \frac{\sigma_3^{(1)}}{2} + \hbar\omega_0 \frac{\sigma_3^{(2)}}{2} + \hbar\omega a^\dagger a + \hbar g(a\sigma_1^\dagger + a^\dagger\sigma_1) + \hbar g(a\sigma_2^\dagger + a^\dagger\sigma_2), \quad (1)$$

where $\sigma_3^{(1)}$ and σ_1^\dagger represent the Pauli matrices for atom number 1 and similarly for atom 2, and g is the atom-field coupling constant. We also assumed that these atoms are in resonance with the cavity field. In the interaction picture, we can write

$$V = \hbar g(a\sigma_1^\dagger + a^\dagger\sigma_1) \otimes 1_2 + \hbar g(a\sigma_2^\dagger + a^\dagger\sigma_2) \otimes 1_1. \quad (2)$$

If the upper and lower levels are denoted by $|a\rangle$ and $|b\rangle$, the system can be described by means of the basis $|a\rangle_1|a\rangle_2$, $|a\rangle_1|b\rangle_2$, $|b\rangle_1|a\rangle_2$, and $|b\rangle_1|b\rangle_2$. On that basis, V is a 4×4 matrix which can be written as

$$V = \hbar g \begin{pmatrix} 0 & a & a & 0 \\ a^\dagger & 0 & 0 & a \\ a^\dagger & 0 & 0 & a \\ 0 & a^\dagger & a^\dagger & 0 \end{pmatrix}. \quad (3)$$

It is not difficult to find the time-evolution operator for this system, since the Hamiltonian is time independent under the above-mentioned conditions. The result is

$$U(\Delta\tau) = \begin{pmatrix} A & -iaS & -iaS & B \\ -iSa^\dagger & D & E & -iSa \\ -iSa^\dagger & E & D & -iSa \\ B^\dagger & -ia^\dagger S & -ia^\dagger S & \bar{A} \end{pmatrix}, \quad (4)$$

where we have defined the different operators in $U(\Delta\tau)$ as follows:

$$A = 1 + \frac{a(C-1)a^\dagger}{\Lambda}, \quad B = \frac{a(C-1)a}{\Lambda}, \quad D = \frac{1}{2}(1+C),$$

$$E = \frac{-1}{2}(1-C), \quad C = \cos(\sqrt{2}g\Delta\tau\sqrt{2\hat{n}+1}), \quad (5)$$

$$S = \frac{\sin(\sqrt{2}g\Delta\tau\sqrt{2\hat{n}+1})}{\sqrt{2}\sqrt{2\hat{n}+1}}, \quad \Lambda = 2\hat{n}+1,$$

$$\bar{A} = 1 + \frac{a^\dagger(C-1)a}{\Lambda},$$

$\Delta\tau$ being the interaction time during which two atoms are present inside the cavity. For the time being, $\Delta\tau$ is considered fixed, but this model will be improved later on introducing some statistical features.

The total density matrix of the system has the following elements:

$$\rho_T = \begin{pmatrix} \rho_{aa,aa} & \rho_{aa,ab} & \rho_{ab,aa} & \rho_{ab,ab} \\ \rho_{aa,ba} & \rho_{aa,bb} & \rho_{ab,ba} & \rho_{ab,bb} \\ \rho_{ba,aa} & \rho_{ba,ab} & \rho_{bb,aa} & \rho_{bb,ab} \\ \rho_{ba,ba} & \rho_{ba,bb} & \rho_{bb,ba} & \rho_{bb,bb} \end{pmatrix}, \quad (6)$$

where the first pair of labels corresponds to atom 1 and the second pair to atom 2. Then, when one partially traces one atom, 1 or 2, we obtain

$$\begin{aligned} \rho_1 &\equiv \text{tr}_2 \rho_T = \sum_{i=a,b} \langle i | \rho_T | i \rangle_2 \\ &= \begin{pmatrix} \rho_{aa,aa} + \rho_{aa,bb} & \rho_{ab,aa} + \rho_{ab,ab} \\ \rho_{ba,aa} + \rho_{ba,bb} & \rho_{bb,ba} + \rho_{bb,bb} \end{pmatrix}, \end{aligned} \quad (7)$$

and similarly

$$\rho_2 = \begin{pmatrix} \rho_{aa,aa} + \rho_{bb,aa} & \rho_{aa,ab} + \rho_{bb,ab} \\ \rho_{aa,ba} + \rho_{bb,ba} & \rho_{aa,bb} + \rho_{bb,bb} \end{pmatrix}. \quad (8)$$

Now let us assume that the atom enters the cavity regularly every $\Delta t_i = \Delta t = \text{const} < \tau_c$, where τ_c is the atomic flight time through the cavity, so that if the process starts at time t_i there will be one atom during a time $\tau_0 = \Delta t_i$ and two atoms during $\Delta \tau = \tau_c - \Delta t_i$. This sequence repeats (Fig. 1).

For the sequence described above, we can write

$$\rho(t_i + \tau_0) = \bar{\rho}(t_i) = \begin{pmatrix} \mathcal{C} \rho_{aa}(t_i) \mathcal{C} + \mathcal{S} a \rho_{bb}(t_i) a^\dagger \mathcal{S} & i \mathcal{C} \rho_{aa}(t_i) \mathcal{S} a - i \mathcal{S} a \rho_{bb}(t_i) \bar{\mathcal{C}} \\ + i \mathcal{C} \rho_{ab}(t_i) a^\dagger \mathcal{S} - i \mathcal{S} a \rho_{ba}(t_i) \mathcal{C} & + \mathcal{S} a \rho_{ab}(t_i) \mathcal{S} a + \mathcal{C} \rho_{ab}(t_i) \bar{\mathcal{C}} \\ - i a^\dagger \mathcal{S} \rho_{aa}(t_i) \mathcal{C} + i \bar{\mathcal{C}} \rho_{bb}(t_i) a^\dagger \mathcal{S} & \bar{\mathcal{C}} \rho_{bb}(t_i) \bar{\mathcal{C}} + a^\dagger \mathcal{S} \rho_{bb}(t_i) \mathcal{S} a \\ + a^\dagger \mathcal{S} \rho_{ab}(t_i) a^\dagger \mathcal{S} + \bar{\mathcal{C}} \rho_{ba}(t_i) \mathcal{C} & + i \bar{\mathcal{C}} \rho_{ba}(t_i) a^\dagger \mathcal{S} - i a^\dagger \mathcal{S} \rho_{ab}(t_i) \bar{\mathcal{C}} \end{pmatrix}, \quad (9)$$

where $\rho(t_i + \tau_0)$ is just the time-evolved version of $\rho(t_i)$ under the Jaynes-Cummings model, with

$$\begin{aligned} \mathcal{C} &= \cos(g\tau_0 \sqrt{\hat{n} + 1}), \\ \mathcal{S} &= \frac{\sin(g\tau_0 \sqrt{\hat{n} + 1})}{\sqrt{\hat{n} + 1}}, \\ \bar{\mathcal{C}}(\hat{n}) &= \mathcal{C}(\hat{n} - 1). \end{aligned} \quad (10)$$

Next, during an interval $\Delta \tau$, there are two atoms in the cavity, that is,

$$\rho_T(t_{i+1}) = U(\Delta \tau) \rho(t_i + \tau_0) \otimes \rho_{\text{atom}} U^\dagger(\Delta \tau). \quad (11)$$

We notice that in Eq. (11) a direct product is formed between $\rho(t_i + \tau_0)$, given by Eq. (9) and the density matrix for the new atom that enters the cavity. The result is a 4×4 matrix if we inject a new atom in its upper state:

$$\rho(t_i + \tau_0) \otimes \rho_{\text{atom}} = \begin{pmatrix} \bar{\rho}_{aa}(t_i) & \bar{\rho}_{ab}(t_i) & 0 & 0 \\ \bar{\rho}_{ba}(t_i) & \bar{\rho}_{bb}(t_i) & 0 & 0 \\ 0 & 0 & 0 & 0 \\ 0 & 0 & 0 & 0 \end{pmatrix}. \quad (12)$$

Next, we proceed to perform the calculation suggested in Eq. (11). At the end of the time period ($\Delta \tau$) an atom of type 2 leaves the cavity. That is, one traces over the second pair of indices, leading to the following result:

$$\begin{aligned} \rho(t_{i+1}) &= \rho(t_i + \tau_0 + \Delta \tau) = \text{tr}_2 U(\Delta \tau) \rho(t_i + \tau_0) \otimes \rho_{\text{atom}} U^\dagger(\Delta \tau) \\ &= \begin{pmatrix} A \bar{\rho}_{aa} A + a S \bar{\rho}_{bb} S a^\dagger & a S \bar{\rho}_{ba} a S + S a^\dagger \bar{\rho}_{ab} S a \\ + i A \bar{\rho}_{ab} S a^\dagger - i a S \bar{\rho}_{ba} A & + i A \bar{\rho}_{aa} a S + i D \bar{\rho}_{bb} S a \\ + S a^\dagger \bar{\rho}_{aa} a S + D \bar{\rho}_{bb} D & + A \bar{\rho}_{ab} E + D \bar{\rho}_{ba} B \\ + i D \bar{\rho}_{ba} a S - i S a^\dagger \bar{\rho}_{aa} D & - i a S \bar{\rho}_{bb} E - i S a^\dagger \bar{\rho}_{ab} B \\ a^\dagger S \bar{\rho}_{ba} a S + S a^\dagger \bar{\rho}_{ab} S a^\dagger & S a^\dagger \bar{\rho}_{aa} a S + a^\dagger S \bar{\rho}_{bb} S a \\ + i B^\dagger \bar{\rho}_{aa} a S + i E \bar{\rho}_{bb} S a^\dagger & + i E \bar{\rho}_{ba} a S + i B^\dagger \bar{\rho}_{ab} S a \\ + B^\dagger \bar{\rho}_{ab} D + E \bar{\rho}_{ba} A & + B^\dagger \bar{\rho}_{aa} B + E \bar{\rho}_{bb} E \\ - i a^\dagger S \bar{\rho}_{bb} D - i S a^\dagger \bar{\rho}_{aa} A & - i S a^\dagger \bar{\rho}_{ab} E - i a^\dagger S \bar{\rho}_{ba} B \end{pmatrix}. \end{aligned} \quad (13)$$

Finally, the matrix elements of the total density matrix, after the atom 2 leaves the cavity, are given by

$$\begin{aligned}
(\rho_{aa}^{i+1})_{n,m} = & \{1 + \alpha_{n+1}(\cos\varphi_{n+1} - 1) + \alpha_{m+1}(\cos\varphi_{m+1} - 1) + \alpha_{n+1}(\cos\varphi_{n+1} - 1)\alpha_{m+1}(\cos\varphi_{m+1} - 1)\}(\bar{\rho}_{aa}^i)_{n,m} \\
& + \frac{1}{4}(\cos\varphi_{m+1})(\cos\varphi_n + 1)(\bar{\rho}_{bb}^i)_{n,m} + i\sqrt{\alpha_{m+1}/2}\sin\varphi_{m+1}\{1 + \alpha_{n+1}(\cos\varphi_{n+1} - 1)\}(\bar{\rho}_{ab}^i)_{n,m+1} \\
& - i\sqrt{\alpha_{n+1}/2}\sin\varphi_{n+1}\{1 + \alpha_{m+1}(\cos\varphi_{m+1} - 1)\}(\bar{\rho}_{ba}^i)_{n+1,m} \\
& + \frac{i}{2}\sqrt{\alpha_m/2}\sin\varphi_m\{1 + \cos\varphi_n\}(\bar{\rho}_{ba}^i)_{n,m-1} - \frac{i}{2}\sqrt{\alpha_n/2}\sin\varphi_n\{1 + \cos\varphi_m\}(\bar{\rho}_{ab}^i)_{n-1,m} \\
& + \frac{1}{2}\sqrt{\alpha_{n+1}\alpha_{m+1}}\sin\varphi_{n+1}\sin\varphi_{m+1}(\bar{\rho}_{bb}^i)_{n+1,m+1} + \frac{1}{2}\sqrt{\alpha_n\alpha_m}\sin\varphi_n\sin\varphi_m(\bar{\rho}_{aa}^i)_{n-1,m-1},
\end{aligned} \tag{14}$$

$$\begin{aligned}
(\rho_{bb}^{i+1})_{n,m} = & \sqrt{\alpha_n/2}\sin\varphi_n\sqrt{\alpha_m/2}\sin\varphi_m(\bar{\rho}_{aa}^i)_{n-1,m-1} + \frac{1}{4}(\cos\varphi_m - 1)(\cos\varphi_n - 1)(\bar{\rho}_{bb}^i)_{n,m} \\
& + \frac{i}{2}\sqrt{\alpha_m/2}\sin\varphi_m(\cos\varphi_n - 1)(\bar{\rho}_{ba}^i)_{n,m-1} - \frac{i}{2}\sqrt{\alpha_n/2}\sin\varphi_n(\cos\varphi_m - 1)(\bar{\rho}_{ab}^i)_{n-1,m} \\
& + i\sqrt{\beta_n\beta_m\alpha_{n-1}}/2\sin\varphi_{m-1}(\cos\varphi_{n-1} - 1)(\bar{\rho}_{ab}^i)_{n-2,m-1} \\
& - i\sqrt{\beta_n\beta_m\alpha_{m-1}}/2\sin\varphi_{n-1}(\cos\varphi_{m-1} - 1)(\bar{\rho}_{ba}^i)_{n-1,m-2} \\
& + \sqrt{\alpha_{n-1}\beta_n\alpha_{m-1}\beta_m}(\cos\varphi_{n-1} - 1)(\cos\varphi_{m-1} - 1)(\bar{\rho}_{aa}^i)_{n-2,m-2} + \sqrt{\beta_n\beta_m}/2\sin\varphi_{n-1}\sin\varphi_{m-1}(\bar{\rho}_{bb}^i)_{n-1,m-1},
\end{aligned} \tag{15}$$

$$\begin{aligned}
(\rho_{ab}^{i+1})_{n,m} = & \frac{(\cos\varphi_m - 1)}{2}\{1 + \alpha_{n+1}(\cos\varphi_{n+1} - 1)\}(\bar{\rho}_{ab}^i)_{n,m} + i\sqrt{\alpha_m/2}\sin\varphi_m\{1 + \alpha_{n+1}(\cos\varphi_{n+1} - 1)\}(\bar{\rho}_{aa}^i)_{n,m-1} \\
& + \frac{\sqrt{\alpha_{n+1}\alpha_m}}{2}\sin\varphi_{n+1}\sin\varphi_m(\bar{\rho}_{ba}^i)_{n+1,m-1} + \frac{\sqrt{\alpha_n\beta_m}}{2}\sin\varphi_n\sin\varphi_{m-1}(\bar{\rho}_{ab}^i)_{n-1,m-1} \\
& - \frac{i}{2\sqrt{2}}\sin\varphi_{n+1}\sqrt{\alpha_{n+1}}(\cos\varphi_m - 1)(\bar{\rho}_{bb}^i)_{n+1,m} - \frac{i}{\sqrt{2}}\sqrt{\alpha_n\alpha_{m-1}\beta_m}\sin\varphi_n(\cos\varphi_{m-1} - 1)(\bar{\rho}_{aa}^i)_{n-1,m-2} \\
& + \frac{\sqrt{\alpha_{m-1}\beta_m}}{2}(\cos\varphi_n + 1)(\cos\varphi_{m-1} - 1)(\bar{\rho}_{ba}^i)_{n,m-2} + i\frac{(\cos\varphi_n + 1)}{2\sqrt{2}}\sqrt{\beta_m}\sin\varphi_{m-1}(\bar{\rho}_{bb}^i)_{n,m-1},
\end{aligned} \tag{16}$$

where $\alpha_n = n/(2n+1)$, $\beta_n = n/(2n-1)$, and $\varphi_n = g\Delta\tau\sqrt{2(2n+1)}$.

Actually, if we want to check these results experimentally, the model with fixed $\Delta\tau$'s alternating with periods of one atom in the cavity is not very realistic. In a typical experiment [4] one has a Poissonian atomic injection with an average injection time $(\Delta\bar{t}) = \frac{1}{8} \times 10^{-2}$ s or $\Delta\bar{t}/\tau_c \sim 15.6$, where $\tau_c \sim 8 \times 10^{-5}$ s is the atomic flight time inside the cavity. 94% of the time there are no atoms in the cavity, 5.4% of the time one atom, and 0.6% of the time two atoms. In order to simulate such an experiment, we assumed that the velocities are fixed with a Poissonian incidence. For a fixed τ_c , we basically have two cases (Fig. 2). The case (i) corresponds to $\Delta t_i > \tau_c$, where we have one atom followed by zero atoms, which under the present experimental conditions would be the most common case. The second case (ii) corresponds to $\Delta t_i < \tau_c$ in which case, starting from zero, a

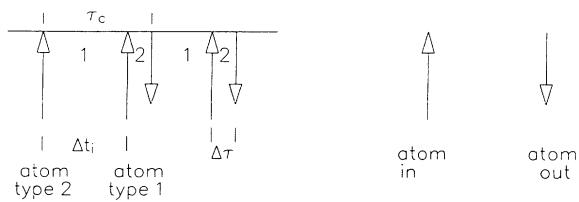


FIG. 1. Periodic sequence of one and two atoms inside the micromaser cavity. The atomic injection here is assumed regular and $\Delta t_i < \tau_c$.

period of one atom is followed by a period of two atoms. If Δt_{i+1} is still less than τ_c , this sequence repeats until the situation reverses, in which case it ends with a period of one atom followed by zero atoms.

III. NUMERICAL RESULTS

We have numerically simulated a Poissonian arrival of atoms for the sequences shown in Fig. 2. For atoms belonging to case (i), which corresponds to the sequence 0-1-0 [Fig. 2(a)], the system evolves with the usual

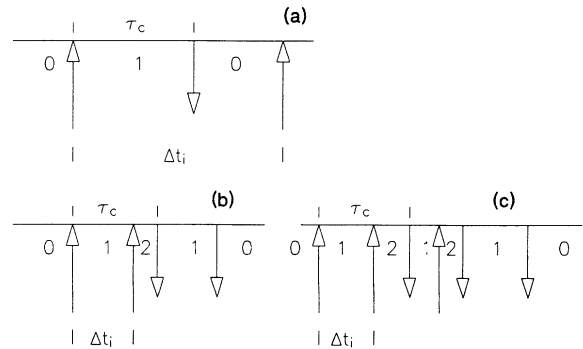


FIG. 2. Poissonian injection of atoms. The upward arrow means an atom enters the cavity and a downward arrow means it leaves. (a) $\Delta t_i > \tau_c$ and we have either zero or one atom inside the cavity. (b) $\Delta t_i < \tau_c$, $\Delta t_{i+1} > \tau_c$. (c) $\Delta t_i < \tau_c$, $\Delta t_{i+1} < \tau_c$, and $\Delta t_{i+2} > \tau_c$.

Jaynes-Cummings model. On the other hand, for atoms belonging to case (ii), possible sequences are 0-1-2-1-0 [Fig. 2(b)] and 0-1-2-1-2-1-0 [Fig. 2(c)]. In these cases the system evolves according to Eqs. (9)–(16). All the sequences start and end with 0 atoms. For a very low beam density, the most probable sequences are 0-1-0. Occasionally, two atoms will be present, and this may occur only once in the time interval τ_c as shown in Fig. 2(b). A more rare case is that in which the two-atom event occurs twice during the time interval τ_c [Fig. 2(c)]. More complicated sequences are very rare in this simulation. However, we have discarded events with three or more simultaneous atoms which of course sets a limitation for extremely high fluxes.

In Fig. 3 the average photon number $\langle n \rangle$ is plotted versus the number of atoms N for $g\tau_c = \pi/\sqrt{3}$, which corresponds to the trapping condition (for a one-photon case) $\sqrt{N_u} + 1g\tau_c = q\pi$, for $q=1$ and $N_u=2$, for $q=2$ and $N_u=11$, etc. The system started at vacuum and in the first region, $N=0-273$, the system quickly went to the $|2\rangle$ state (atoms are injected in the upper level, so the trapping state is a pure $|n\rangle$ state). After $N=274$, a two-atom event occurred (0-1-2-1-0). This provoked a leak in the $N_u(q=1)=2$ trapping block and some probability crossed over to $n=3, 4, \dots$, continuing upward in n until it stopped at the next upward trap, $N_u(q=2)=11$. The linear increase in $\langle n \rangle$ shows this probability flow to $N_u(q=2)=11$. The next flat region implies that we reached a state $\rho \approx 0.9249|2\rangle\langle 2| + 0.075|11\rangle\langle 11|$, which gives precisely the $\langle n \rangle$ in the figure. This probability 0.75 flowed originally $n=2$ to $n=3$ in a two-atom event and after some time reached $n=11$. The remainder of the evolution is similar. It describes the slow probability diffusion through the n space, from one trapping block to the next. In Fig. 4 we plotted $(\Delta n)^2$ vs N and it just confirms the previous interpretation.

Now we increase our beam intensity to $\Delta\bar{t}/\tau_c \sim 15.6$, taking a typical experimental value. In Fig. 5 we observe a little of the steplike features shown before, although

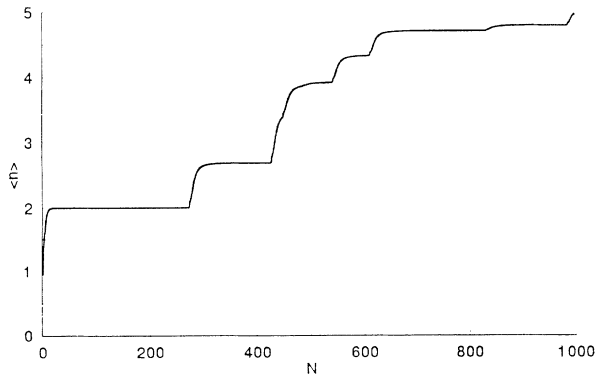


FIG. 3. $\langle n \rangle$ vs N (number of atoms) for a low-density atomic beam, $\Delta\bar{t}/\tau_c = 150.7$ and $N_u(q=1)=2$; that is, $g\tau_c = \pi/\sqrt{3}$. The various “linear” increases start with a two-atom event. The curves become flat again when the probability that escaped from the block q ends in $N_u(q+1)$. The beam has a Poissonian distribution.

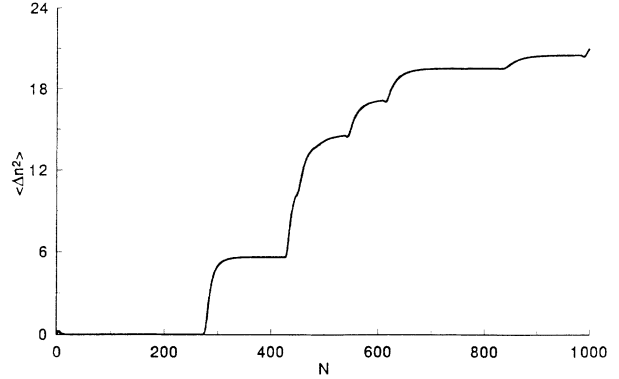


FIG. 4. $\langle (\Delta n)^2 \rangle$ vs N (numbers of photon atoms). The probability diffusion also appears here as a steady increase in $\langle (\Delta n)^2 \rangle$.

here the steps are rather short because the two-atom events are more frequent and the field never quite makes it for the trapping state. In this case we took $N_u(q=1)=2$ and observed a new feature, the appearance of spikes. Numerically, they appear every time there is a sequence 0-1-2-1-2-1-0; that is, the two-atom events appear twice. The explanation is rather simple. The first 0-1-2 sequence produces a probability leak between the upper end of the trapping block q and the downward trapping of the next block $q+1$, that is,

$$N_d(q+1) = N_u(q) + 1. \quad (17)$$

This event, of course, increases $\langle n \rangle$, but now another 1-2-1-0 sequence is present. At this point, we have to remember that the downward trapping condition of the $(q+1)$ block is also bypassed by the *two-photon events*. In other words, the $(q+1)$ block also leaks downward, producing this time a decrease in $\langle n \rangle$. In Fig. 6, we selected a bigger $N_u=50$ or a shorter interaction time $g\tau_c = \pi/\sqrt{51}$. Here we observed that the leakage is practically continuous. The steplike features are gone and the

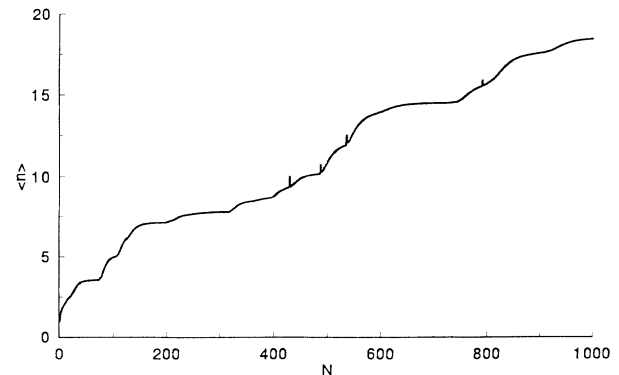


FIG. 5. $\langle n \rangle$ vs N (number of atoms) for a beam density characterized by $\Delta\bar{t}/\tau_c = 15.6$ and $N_u(q=1)=2$, or $g\tau_c = \pi/\sqrt{3}$. The steps are shorter due to the higher frequency of two-atom events. The spikes appear when the 1-2 sequence repeats twice.

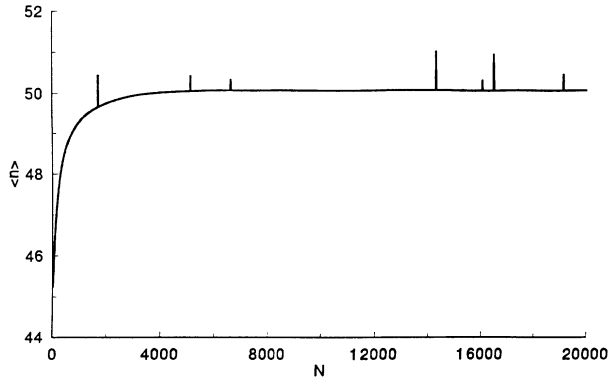


FIG. 6. $\langle n \rangle$ vs N (number of atoms) for $\Delta\bar{F}/\tau_c = 15.6$ and $N_u(q=1) = 50$. The steps are gone and replaced by a slow but continuous increase. The curve looks similar to a normal trapping state curve, except for the spikes and the fact that $\langle n \rangle$ is slightly above 50 for $N = 20\,000$.

curve looks very similar to a trapping state curve, except for the spikes and the fact that $\langle n \rangle$ in the flat region is slightly higher than 50. Figure 7 shows that only at the beginning we have pure $|n\rangle$ state, but after $N = 2\,000$, $\langle (\Delta n)^2 \rangle$ shows a continuous increase.

IV. DISCUSSION

We studied, in this work, the collective effects on the trapping states in a one-photon micromaser. We find that for small photon numbers (N_u), these states could be difficult to detect experimentally for both low and higher beam intensities. However, this situation improves as N_u gets larger, and for $N_u = 50$ the behavior of $\langle n \rangle$ does not

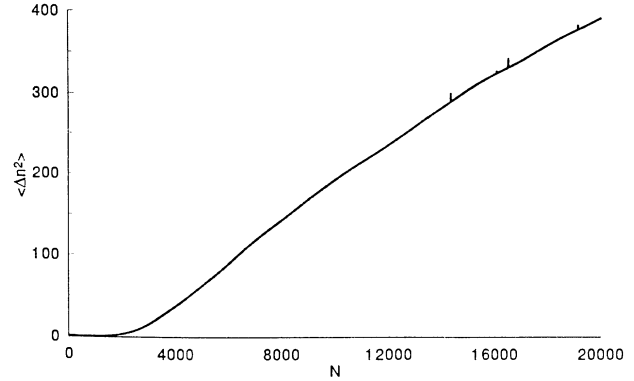


FIG. 7. $\langle (\Delta n)^2 \rangle$ vs N (numbers of photon atoms) for the same parameters as in Fig. 6.

look too different from the usual trapping state, except for the spikes and that the plateau is reached slightly above 50. As a matter of fact, a plateau is never reached. Instead, this is a curve that increases very slowly due to the long time it takes for the probability to diffuse from the lower to the upper end of the trapping block, which is now quite large.

Finally, losses have not been considered here [6,7]. Probably, its effect would be to increase the probability diffusion to the trapping blocks. This and the effects of the atomic measurements on the trapping states [5,8] will be the subject of a future publication.

ACKNOWLEDGMENT

This work is supported in part by the Fondecyt (Chile), Grant Nos. 1930568, 1930564, and 1930159.

-
- [1] R. Bonifacio, G. M. D'Ariano, R. Seno, and N. Sterpi, *Phys. Rev. A* **47**, 2464 (1993).
 - [2] For one-photon trapping states, see, for example, P. Filipowicz, J. Javanainen, and P. Meystre, *J. Opt. Soc. Am. B* **3**, 906 (1986).
 - [3] For two-photon trapping states, see M. Orszag, R. Ramirez, J. C. Retamal, and L. Roa, *Phys. Rev. A* **45**, 6717 (1992).
 - [4] D. Meschede, H. Walther, and G. Muller, *Phys. Rev. Lett.*

- 6**, 551 (1985).
- [5] J. Krause, M. O. Scully, and H. Walther, *Phys. Rev. A* **34**, 2032 (1986).
- [6] L. Roa, J.C. Retamal, and C. Saavedra, *Phys. Rev. A* **47**, 620 (1993).
- [7] M. Orszag, L. Roa, and R. Ramirez, *Phys. Rev. A* **48**, 000 (1993).
- [8] M. Orszag and R. Ramirez, *Opt. Commun.* **101**, 377 (1993).